Est. 1984

ORIENTAL JOURNAL OF CHEMISTRY
An International Open Access, Peer Reviewed Research Journal

www.orientjchem.org

ISSN: 0970-020 X
CODEN: OJCHEG
2023, Vol. 39, No.(2):
Pg. 446-451

Polyaniline-mixed Metal (Fe-Mn-Zn) Oxide Nanocomposite Adsorbent for Removing Cu(II) ions from Aqueous Matrices

SURBHI SANKHLA[1], KAPIL GEHLOT[2]* and DESHRAJ SHARMA[3]

[1]Department of Chemistry, Jai Narain Vyas University, Jodhpur, India.
[2]Department of Chemistry, Lachoo Memorial College of Science & Technology, Jodhpur, Rajasthan, India.
[3]Department of Physics, Lachoo Memorial College of Science & Technology, Jodhpur, Rajasthan, India.
*Corresponding author E-mail: gkapil23@gmail.com

http://dx.doi.org/10.13005/ojc/390225

(Received: December 27, 2022; Accepted: March 20, 2022)

ABSTRACT

A polyaniline-mixed metal (Fe-Mn-Zn) oxide (PANFMZO) nanocomposite adsorbent is synthesized and characterized by FTIR, SEM, SEM/EDX and Brunauer–Emmett–Teller (BET) analysis. Efficiency of PANFMZO as adsorbent for removal of Cu(II) ions from aqueous matrices is analysed. The parameters like change in amount of adsorbent, contact time, pH and initial Cu(II) ion concentration are studied and removal of 69.20% of Cu(II) ion from test solution is achieved. The maximum adsorption capacity of PANFMZO for Cu(II) is found to be 75.1879 mg/g. The adsorption results are described by both Langmuir and Freundlich isotherms, the data fits better with Freundlich isotherm (R^2=0.9998).

Keywords: Nanocomposite, Batch mode technique, Polyaniline, Adsorption

INTRODUCTION

Copper is an essential trace nutrient; however, the excess amount is hazardous to both humans and animals.[1] Due to the numerous industrial and commercial uses of copper metals and compounds[2-4], copper pollution has become a significant environmental issue. The commonly employed techniques for remediation of copper ions[5] from aquatic samples include chemical precipitation[6], flotation[7], biosorption[8-10], electrolytic recovery[11], membrane separation[12], metal adsorption onto minerals[13] and activated carbon[14]. The adsorption process has been extensively studied in order to solve the problem of copper ions contamination in aqueous matrices. Polyaniline-based composites, which are made by combining polyaniline with one or more similar or dissimilar materials, have been reported to be good adsorbents for removing metal ions[15]. Few advantages associated with them include simple synthesis, inexpensive monomer cost, good environmental stability, easily controlled reversible properties by doping, charge exchange and protonation, distinctive functional groups (e.g. -NH-), and tunable properties[16]. The diverse morphological structures, high surface areas, good dispersibility, and synergistic features of the polymer and the filler make PANI-based nanocomposites suitable candidates for the adsorption of metal ions[17]. In this work, polyaniline-formaldehyde copolymer has been synthesized and employed for remediation of Cu(II) ions from aqueous matrices in the range of its toxicity limit.

MATERIAL AND METHOD

To prepare PANFMZO, 10.0 mL (100 mmol) of aniline was acidified with 12.0 mL (120 mmol) of concentrated HCl, the anilinium salt obtained was dissolved in 50.0 mL of water. 10.0 mL (100 mmol) of formaldehyde was added to the above solution and the copolymer obtained was cooled to room temperature. Aqueous solution of $FeCl_3.6H_2O$, $MnCl_2.4H_2O$ and $ZnCl_2$, in different molar ratios (Table 1) was mixed slowly in the copolymer with constant shaking over sonicating bath. Resulting mixture was treated with 10% NaOH with constant shaking for 10 min and precipitate was allowed to settle down for 45 minute. The precipitate was vacuum filtered and washed until free from alkali and dried at 70°C to get PANFMZO nanocomposite in powder form. 1000 ppm stock solution of Cu(II) ion was prepared by using standard method as reported[18].

Table 1: Molar ratios of Fe(III), Mn(II) and Zn(II) for synthesis of PANFMZO

S. No	Sample	Moles of Fe(III) ions	Moles of Mn(II) ions	Moles of Zn(II) ions
1	S1	0.04	0.0189	0.0000
2	S2	0.04	0.0151	0.0039
3	S3	0.04	0.0113	0.0079
4	S4	0.04	0.0075	0.0119
5	S5	0.04	0.0037	0.0159
6	S6	0.04	0.0000	0.0199

PANFMZO was shaken with the Cu(II) ion solution in a stoppered conical flask and the concentration of residual ions was determined using AAS (ECIL, AAS4141) and the concentration of Cu(II) ion adsorbed, q_e (mg/L), was determined using following equation[19]

$$q_e = \frac{(C_o - C_e)V}{W}$$

Where c_o and c_e: initial and equilibrium concentrations of adsorbate (mg/L), respectively, V: volume of solution (L) and W: mass of adsorbent (g). The percentage removal of Cu(II) ions was determined using following equation:

$$\% \text{ removal} = \frac{C_o - C_e}{C_o} \times 100\%$$

RESULTS AND DISCUSSION

IR spectroscopy was employed to determine the changes in the vibrational frequencies of the groups present in PANFMZO due to adsorption of Cu(II) ion. PANFMZO before adsorption showed a peak at 3287.5 cm^{-1} due to secondary N-H stretch, while peak at 2791.8 cm^{-1} indicated formaldehyde -CH_2 moiety. C-N aromatic stretch at 1338.1 cm^{-1} further confirmed the amine and a peak at 1599.0 cm^{-1} indicated C=C stretch of aromatic ring. Peak at 827.5 cm^{-1} appeared due to C-H out of plane bending and busy finger print region was due to substitution at 1 and 4 positions of the benzene ring (Figure 1a)[20].

After adsorption, the IR spectra showed marked variation in the major peaks. The shifted peaks were observed at 3350.9 cm^{-1} (N-H stretch), 2899.9 cm^{-1} (C-H stretch; aliphatic), 1341.8 cm^{-1} (C-N aromatic stretch), 1587.8 cm^{-1} (C=C stretch; aromatic), 816.3 cm^{-1} (C-H bending) and changes in the finger print region were also observed (Figure 1b)[21].

The SEM image revealed porous structure of material with irregular shaped nanoparticles of size ranging from 72.03 nm to 133 nm (Fig. 2a). SEM-EDX analysis clearly indicated presence of only Fe, Mn, Zn and O showing the formation of the oxides of the metal ions and peak of C was due to presence of the polymer matrix (Figure 2b).

SEM image (Fig. 3a) after adsorption studies revealed rugged morphology with filled pores indicating the presence of adsorbed Cu(II) ions. This was further confirmed by SEM-EDX which showed additional peak of Cu along with Fe, Mn, Zn and O (Fig. 3b). The mapping image also provided additional evidence for the adsorption of Cu with its uniform distribution throughout the surface of PANFMZO (Figure 3c).

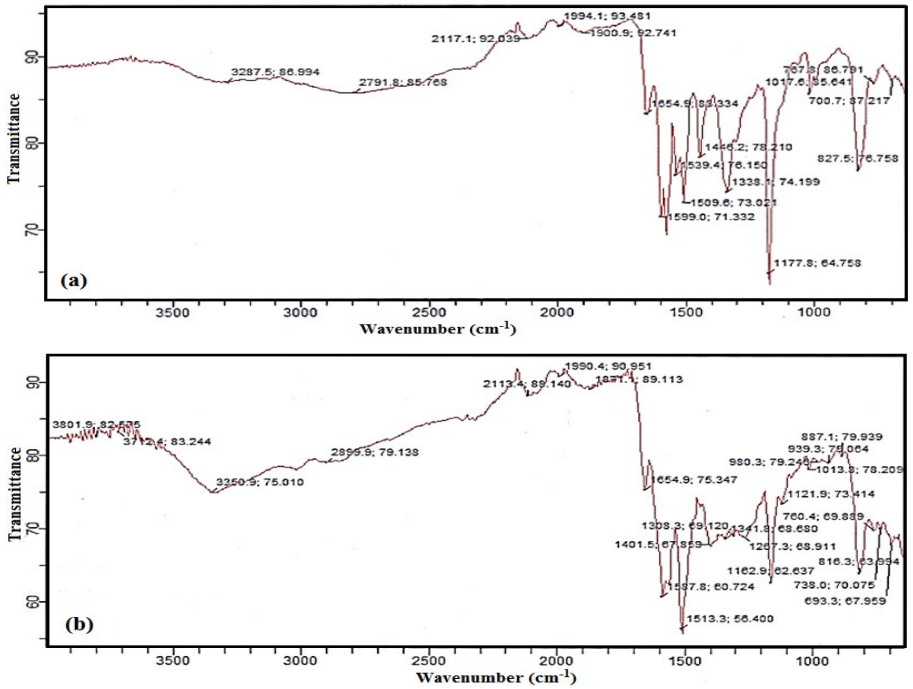

Fig. 1. IR spectrum of (a) PANFMZO (b) PANFMZO after adsorption

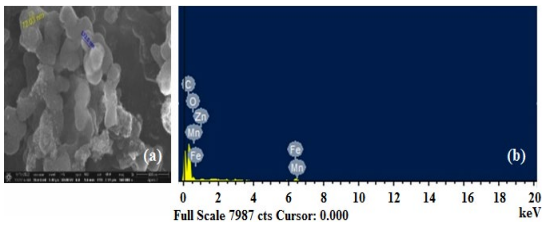

Fig. 2. (a) SEM Image (b) SEM-EDX of PANFMZO before Cu(II) ion adsorption

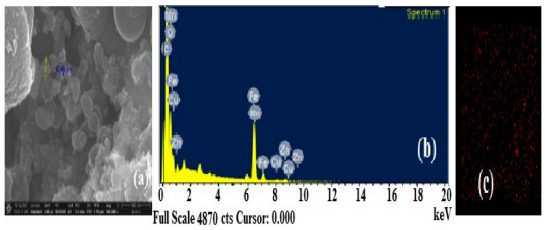

Fig. 3. (a) SEM Image (b) SEM-EDX (c) SEM-EDX mapping of copper after Cu(II) ion adsorption

From preliminary adsorption experiments, the distribution coefficient value (K_d) for samples, S1, S2, S3, S4, S5 and S6 were found to be 3502.85, 4877.45, 1584.47, 901.46, 812.71 and 632.53, respectively. Sample S2 (molar ratios Fe(III): Mn(II): Zn(II): 2.65:1.00:2.58) showed maximum K_d value and therefore was selected for further studies. The equilibrium data was calculated with the help of batch methodology[22] and optimum conditions for Cu(II) ion adsorption using PANFMZO were analyzed by studying domains like variation in pH, adsorbent dose, time of contact and initial concentration of adsorbate. To examine the effect of dose, 0.01 to 0.07 g of PANFMZO was shaken with 250 mL of 1mg/L solution of Cu(II) ion Cu(II) ion adsorption increased with rise in amount of PANFMZO up to 0.05 g (Fig. 4a). This may be ascribed to upsurge in available adsorption sites, however, further increase in dose did not show any change due to aggregation of adsorbent[23]. The Cu(II) ion adsorption was also monitored by varying the contact time from 10–60 min (Fig. 4b). The initial rise in adsorption was observed with time and the equilibrium was attained after 40 minute. Thereafter insignificant change in Cu(II) ion adsorption indicated that the adsorption sites are saturated with Cu(II) ions. To optimize pH conditions, Cu(II) ion adsorption studies were executed from pH 1 to 7. At pH 6, maximum adsorption was observed, at lower pH values the H^+ seems to compete with metal ion for the adsorption. At pH>6 the solution started showing precipitation which may be due to complexation of Cu(II) ions with OH^- ions (Fig. 4c). The optimum initial concentration of adsorbate was also analyzed (Fig. 4d). The percentage removal of Cu(II) ions at 0.8, 1.0, 1.5, 2.0, 2.5, 3.0 mg/L was found to be 69.12%, 69.20%, 68.33%, 67.75%, 67.40% and 67.00%, respectively. The percentage removal decreases beyond 1.0 mg/L which indicated that adsorption sites are saturated beyond this concentration.

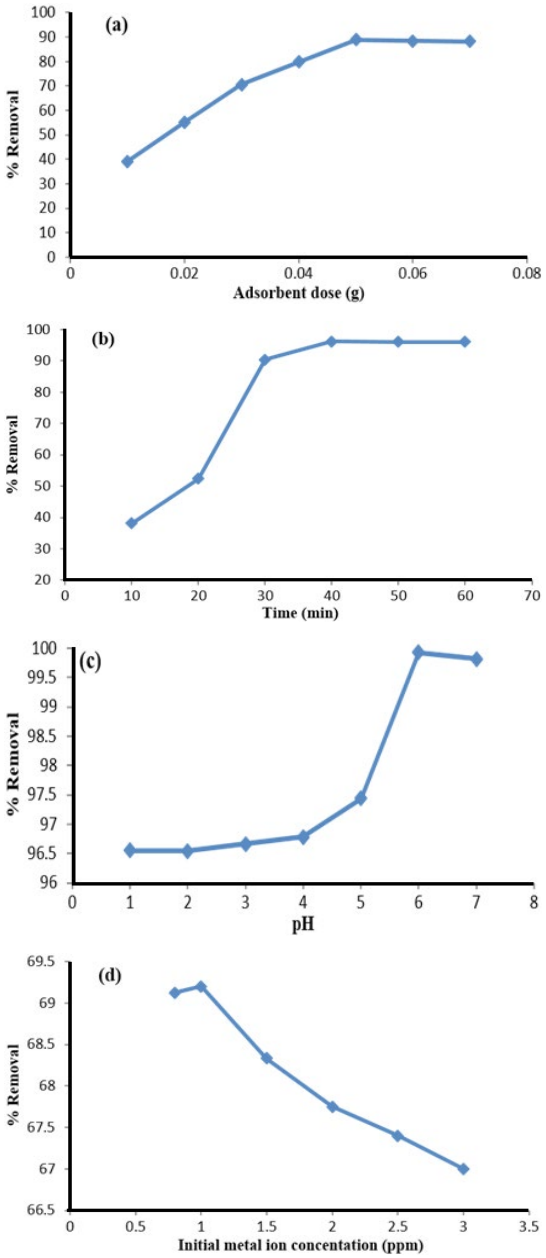

Fig. 4. Effect of (a) PANFMZO dose (b) contact period (c) pH (d) initial metal ion concentration

The obtained data for Cu(II) ion adsorption was validated using Langmuir[24] and Freundlich isotherms[25].

Langmuir isotherm was linear (Fig. 5a) with q_m and R_L values 75.1879 mg/g and 0.8659, respectively. The value of R_L less than 1 indicated favourable adsorption of the Cu(II) ions on the adsorbent. Even the Freundlich isotherm (Fig. 5b) was found to be linear with n and K_f values being 1.0817 and 8.5704 mg/g. The n value was found to be greater than one but less than 10 indicating favourable adsorption of Cu(II) ions on PANFMZO. The R^2 value for both Langmuir and Freundlich adsorption isotherm were high. Higher value of regression correlation coefficient of Freundlich model (R^2=0.9998) indicated that adsorbed Cu(II) ions forms multilayer onto the adsorbent surface.

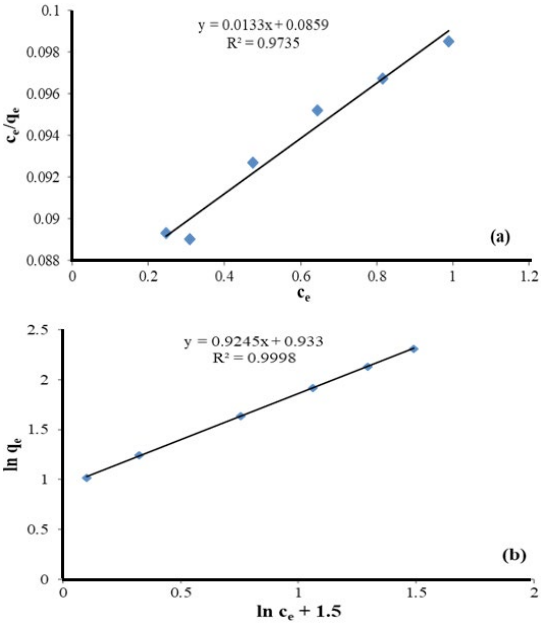

Fig. 5. (a) Langmuir and (b) Freundlich adsorption isotherm

To investigate the surface area and porosity of PANFMZO, BET analysis was performed by adsorption-desorption of N_2 (Fig. 6). The surface area and the average pore diameter of PANFMZO was found to be 12.06 m^2/g and 43.98 Å, respectively.

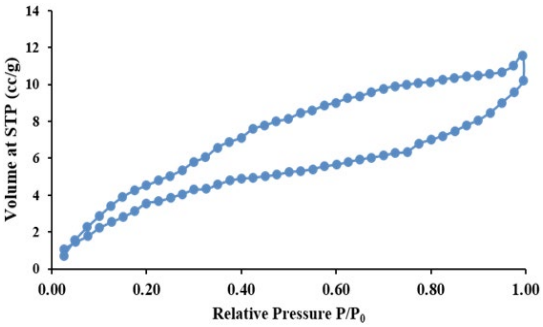

Fig. 6. Nitrogen adsorption-desorption isotherm of PANFMZO

The adsorption capacity of PANFMZO (75.1879 mg/g) is comparable to the reported values in literature as shown in Table 2.

Table 2: Maximum adsorption capacity for Cu(II) ions by different adsorbents

S. No	Adsorbent used for removal of Cu(II) ions	Adsorption capacity q_m (mg/g)	References
1	Polyaniline graft chitosan beads	100	[26]
2	Polyaniline/Clay nanomaterials	22.7	[27]
3	PANI calcium alginate	67.95	[28]
4	Chitosan Grafted with Polyaniline	131.58	[29]
5	Prussian blue/polyaniline@cotton fibers composite	31.93	[30]
6	Phytic acid-doped polyaniline nanofibers	5.29	[31]
7	Polyaniline/Ferricyanide composite	41.625	[32]
8	Polyanilne	38.265	[33]
9	Polyaniline-wheat husk composite	95	[34]
10	Current Study	75.1879	-

CONCLUSION

PANFMZO nanocomposite synthesized by the chemical oxidation method was used as adsorbent for removing Cu(II) ion in aqueous matrices. With 0.05 g adsorbent dose, contact period of 40 min, at pH 6, and 1mg/L of Cu(II) ion concentration, 69.2% of Cu(II) ions were removed and adsorption capacity, q_m of PANFMZO was found to be 75.1879 mg/g. Adsorption isotherm shows that the experimental data satisfy Freundlich isotherm better than Langmuir isotherm.

ACKNOWLEDGMENT

Authors acknowledge Department of Chemistry, Jai Narain Vyas University, Jodhpur and IIT Jodhpur for instrumental analysis.

Conflict of interest

Authors declare no conflict of interest for this work.

REFERENCES

1. Emenike, E. C.; Adeniyi, A.G.; Omuku, P.E.; Okwu, K.C.; Iwuozor, K. O. *J. Water Process Eng.*, **2022**, *47*, 102715.
2. Kilany, A.Y.; Nosier, S.A.; Hussein, M.; Abdel-Aziz, M.H.; Sedahmed, G.H. *Sep. Purif. Technol.*, **2020**, *248*, 117056.
3. Davamani, V.; Parameshwari, C.I.; Arulmani, S.; Ezra John, J.; Poornima, R. *J. Environ. Chem. Eng.*, **2021**, *9*, 105528.
4. Amélie, J.; Lucie, C.; Guy, M.; Jean F. B. *J. Clean. Prod.*, **2021**, *279*, 123687.
5. Phuengphai. P.; Singjanusong. T.; Kheangkhun. N.; Wattanakornsiri. A. *Water Sci. Eng.*, **2021**, *14*, 286–294.
6. Chen, Q.; Yao. Y.; Li. X.; Lu.J.; Zhou. J.; Huang. Z. *J. Water Process. Eng.*, **2018**, *26,* 289–300.
7. Wu, H.; Wang, W.; Huang, Y.; Han, G.; Yang, S.; Su, S.; Sana, H.; Peng, W.; Cao. Y.; Liu. J. *J. Hazard. Mater.*, **2019**, *371*, 592–602.
8. Dusengemungu, L.; Kasali, G.; Gwanama, C.; Ouma, K. O. *Front. Microbiol.*, **2020**, *11*, 582016.
9. Bashir, A.; Malik, L. A.; Ahad, S.; Manzoor. T.; Bhat, M. A.; Dar, G. N. *Environ. Chem. Lett.*, **2019**, *17*, 729-754.
10. Villen-Guzman, M.; Gutierrez-Pinilla, D.; Gomez-Lahoz, C.; Vereda-Alonso, C.; Rodriguez-Maroto, J. M.; Arhoun, B. *Environ. Res.*, **2019**, *179*, 108849.
11. Xiaoxia, Y.; Yaping, Q.; Feifan, L.; Jiancheng, S.; Zhi, S.; Shuhui, S.; Mengjun, C.; Shengyan, P. *Waste Manage.*, **2019**, *95*, 370-376.
12. Duan, H.; Liu, H.; Hu, C.; Yang, X.; Wang, X. *RSC Adv.*, **2020**, *10*, 18860.
13. Komy, Z. R.; Shaker, A. M.; Heggy, S. E. M.; El-Sayed, M. E. A. *Chemosphere.*, **2014**, *99*, 117-124.
14. Chen, W. S.; Chen, Y. C.; Lee, C. H. *Processes.*, **2022**, *10*, 150.
15. Eskandari, E.; Kosari, M.; Farahani, M.H.D.A.; Khiavi, N.D.; Saeedikhani, M.; Katal, R.; Zarinejad, M. *Sep. Purif. Technol.*, **2019**, *231*, 115901.
16. Zare, E. N.; Motahari, A.; Sillanpää, M. *Environ. Res.*, **2018**, *162*, 173-195.
17. Samadi, A.; Xie, M.; Li, J.; Shon, H.; Zheng, C.; Zhao, S. *Chem. Eng. J.*, **2021**, *418*, 129425.
18. Rice. E.W.; Baird. R.B.; Eaton. A.D.; Clesceri. L.S. Standard Methods for the Examination of Water and Wastewater 22nd Edition., **2012**, 3-74.

19. Primo, J.O.; Bittencourt, C.; Acosta, S.; Sierra-Castillo, A.; Colomer, J.F.; Jaerger, S.; Teixeira, V.C.; Anaissi, F.J.; *Front Chem*., **2020**, *8*, 571790.
20. Pavia, D.; Lampman, G.; Kriz, G. Introduction to Spectroscopy, a Guide for Students of Organic Chemistry. 8th Indian Reprint, Brooks/Cole, Cengage Learning., **2011**, 51-53.
21. Ajithkumar, M.; Arivoli, S. *Orient. J. Chem*. **2021**, *37*, 1324-1328.
22. Ramutshatsha, D.; Ngila, J.C.; Ndungu, P.G.; Nomngongo, P.N. Desalin. *Water Treat.*, **2018**, *104*, 206–216.
23. Mishra, A. K.; Shahi, V. K.; Agrawal, N. R.; Das, I.; *J. Chem. Eng. Data.,* **2018**, *63*, 3206–3214.
24. Wang, L.; Shi, C. X.; Wang, L.; Pan, L.; Zhang, X. W.; Zhou, J. *J. Nanoscale*., **2020**, *12*, 4790-4815.
25. Sun. H.; Xia. N.; Liu. Z.; Kong. F.; Wang. S. *Chemosphere*., **2019**, *236*, 124370.
26. Igberase, E.; Osifo, P.; Ofomaja, A. *J. Environ. Chem. Eng*., **2014**, *2*(1), 362–369.
27. Soltani, H.; Belmokhtar, A.; Zeggai, F. Z.; Benyoucef, A.; Bousalem, S.; Bachari, K. *J. Inorg. Organomet. Polym. Mater*., **2019**, *29*(3), 841–850.
28. Jiang, N.; Xu, Y.; Dai, Y.; Luo, W.; Dai, L. *J. Hazard. Mater*., **2012**, *215–216*, 17–24.
29. Zare, H.; Taleghani, H. G.; Khanjani, J. *Int. J. Eng. Trans. B Appl*., **2021**, *34*(2), 305–312.
30. Wang, X.; Li, Q.; Yang, D.; An, X.; Qian, X. *Coatings.,* **2022**, *12*(2), 138.
31. Kim, H. J.; Im, S.; Kim, J. C.; Hong, W. G.; Shin, K.; Jeong, H. Y.; Hong, Y. *J. ACS Sustain. Chem. Eng*., **2017**, *5*(8), 6654–6664.
32. Ahmad Rafiqi, F.; Majid, K. *J. Environ. Chem. Eng*., **2015**, *3*(4), 2492–2501.
33. Arsalan, M.; Siddique, I.; Awais, A.; Baoji, M.; Khan, I.; Badran, M.; Mousa, A. A. A. *Front. Environ. Sci*., **2022**, *10, 895463*..